AGRICULTURAL WATER MANAGEMENT 88 (2007) 99–109

available at www.sciencedirect.com

journal homepage: www.elsevier.com/locate/agwat

Monitoring irrigation performance in Esfahan, Iran, using NOAA satellite imagery

Mehdi Akbari [a,*], *Norair Toomanian* [b], *Peter Droogers* [c], *Wim Bastiaanssen* [c], *Ambro Gieske* [c]

[a] *Agricultural Engineering Research Institute, PO Box 31585-845, Karaj, Iran*
[b] *Esfahan Agricultural Research Center, PO Box 81785-19, Esfahan, Iran*
[c] *International Water Management Institute, PO Box 2075, Colombo, Sri Lanka*

ARTICLE INFO

Article history:
Accepted 10 October 2006
Published on line 4 December 2006

Keywords:
Irrigation performance
Evapotranspiration
Biomass production
Water productivity
Remote sensing
Esfahan
Iran

ABSTRACT

Performance of four irrigation systems in the Zayandeh Rud Basin, Esfahan, Iran, was assessed for the systems as a whole, rather than on only official registered water extractions and uses. NOAA satellite images were analyzed using the SEBAL (surface energy balance algorithm for land) algorithm to obtain actual and potential evapotranspiration and biomass production. The missing term in the water balance was used to estimate groundwater extractions and unaccounted extraction from the river. For Abshar-Left groundwater extraction surpassed surface water applications, while for Nekouabad-Left groundwater extractions were very low. For Abshar-Right a large amount of water was pumped directly out of the river. The assessment of the systems was expressed by the productivity of water, defined as kg biomass over m^3 water evaporated. Productivity was higher ($\sim$0.72 kg m^{-3}) for the systems relying on surface water (Nekouabad-Left and Abshar-Right) than for the conjunctive systems, reflecting the difference in water quality between groundwater and surface water. Finally, it was concluded that the advantages of the methodology presented here over the traditional assessments are: (i) most data is readily available, (ii) all water users are included, (iii) groundwater extraction can be estimated, and (iv) a real time assessment can be setup using this approach.

1. Introduction

Increasing pressure on water resources requires a sound knowledge of where, when and how much water is used. Agriculture, and especially irrigated agriculture, is the main global water consumer and, consequently, a more productive use in this sector will have a large impact. Moreover, it is estimated that by 2025 cereal production will have to increase by 38% to meet world food demands (Seckler et al., 1999), putting even more stress on the scarce water resources.

Increasing food production with limited water resources is the main challenge for the irrigated agriculture sector in the 21st and, therefore, monitoring the irrigation performance is meaningful. The term of ‘‘irrigation performance’’ for different irrigation level (field, irrigation system and basin) can be quantified by factors such as water inflows and outflows, crop demand (net irrigation water requirement), water use, system losses, crop production and the extent cultivated. Assessing the irrigation performance is necessary in evaluating impacts of field-level agricultural and hydrological interventions. The procedure for analyzing the use, depletion and productivity of water is termed water accounting which considers components of the water balance and classifies them according to uses and the productivity of these uses (Molden and Sakthivadivel, 1999). The ultimate objective of the performance assessment is to achieve effective and efficient

* *Corresponding author*. Tel.: +98 261 27053020/2708359; fax: +98 261 2706277.
E-mail address: Akbari_m43@yahoo.com (M. Akbari).
0378-3774/$ – see front matter © 2006 Published by Elsevier B.V.
doi:10.1016/j.agwat.2006.10.019

performance of the institution by providing relevant feedback to the management at all levels. Time series of indicators and rates of change are commonly used in these assessments (Bos, 1997). Performance of irrigated agriculture has been expressed in terms of efficiencies based on observed flows in different points in the water distribution system, such as reservoir releases, main, secondary and tertiary canal, field, and plant. The ratio of the flow at a lower level to the flow at a higher level defines the efficiency of that particular part of the system. For example, the ratio of total water received at the field by farmers over the water releases from a reservoir is defined as the system efficiency. Similar, the ratio of total evapotranspiration on a particular field over water delivered to that field is defined as the application efficiency. The main objective of irrigation engineering has always been to increase those efficiencies. A serious drawback of this approach is that water considered as a loss, indicated by a low efficiency, is not a real loss but is often used somewhere else. This ‘‘lost’’ water is likely to be used by downstream users, or percolating to the groundwater, or used for ‘‘illegal’’ irrigation activities. In other words, increasing efficiencies requires additional water deliveries to the previous users of this ‘‘lost’’ water.

To overcome these problems with efficiencies, Molden and Sakthivadivel (1999) described a conceptual framework for water accounting, based on inflows and outflows. The framework includes the assessment of system performance in terms of the water productivity (PW), defined as the amount of water used to produce 1 kg of crop. Different WP were identified, based on different definitions of water used. Here we apply only $WP_{process\ depletion}$, which refers to the amount of water evapotranspirated to produce 1 kg of crop. A practical example of the use of other WP can be found elsewhere (Droogers and Kite, 1999, 2001). Evapotranspiration is an important factor in water productivity and monitoring irrigation performance. However, direct measurement of actual evapotranspiration is difficult and, at best, mostly provides point values. At present, in most cases, satellite remote sensing data have been used for estimating potential and actual evapotranspiration at regional scale. Many researchers have worked on developing models that accept remote sensing data as input to estimate potential evaporation (e.g. Menenti and Azzali, 1992; Choudhury, 1997) and actual evaporation (e.g. Nieuwenhuis et al., 1985; Pelgrum and Bastiaanssen, 1996). Main advantage of this approach is that large areas are covered, and that data is easily obtainable without extensive monitoring networks in the field (Bandara, 2003; Chemin et al., 2004). The estimation of evapotranspiration using remote sensing data for irrigation performance requires the routine processing of images on a near-real-time basis. The availability of advanced very high resolution radiometer (AVHRR) imagery from NOAA series meteorological satellites on daily basis at most of the national meteorological services worldwide at no extra cost, makes them a viable alternative to estimate irrigated area, actual and potential evapotranspiration and water productivity for performance of irrigation systems and devise better management.

In summary the objectives of this study: (i) use satellite images to estimate irrigated area, actual and potential evapotranspiration and biomass yields, (ii) estimate the performance of irrigation systems based on this information, and (iii) estimate groundwater extraction as the closing term of the water balance.

2. Materials and methods

2.1. Study area

The main irrigated areas in the Zayandeh Rud Basin, Esfahan, Iran, 41,500 km^2, have been selected to analysis the performance of major irrigation systems (Fig. 1). The main river of the Zayandeh Rud Basin, runs for some 350 km roughly west-east from the Zagros Mountains to the Gavkhuni Swamp. The majority of the basin is a typical arid and semi-arid desert.

The gross command area of the main systems is about 135,000 ha, while net command area is about 92,000 ha. Cropped area is between 70 and 80%. Main winter crops are wheat and barley (November–May/June), summer crops are rice (June–October) and vegetables (March–October). Perennial crops encompass orchards and alfalfa. Rainfall is very limited, around 130 mm year^{-1}, most occurring in the winter months from December to April. Temperatures are hot in summer, reaching an average of 30 °C in July, but are cool in winter dropping to an average minimum temperature of 3 °C in January. In the region, a water management project was performed between 1998 and 2002. The main purpose of the project was to foster integrated approaches to managing water resources at basin, irrigation system and farm levels, and thereby contribute to promoting and sustaining agriculture in the country. Therefore, monitoring the irrigation performance is meaningful. Detailed description of the study area can be found in Murray-Rust et al. (2000).

2.2. Data and methodology

A set of 40 NOAA-14 images were downloaded from the satellite active archive's website (http://www.saa.noaa.gov). These local area coverage (LAC) images have a spatial resolution of 1 km at nadir, with Level 1B File Format. Many remote sensing packages (Erdas, PCI) have standard import options for this type of files. For ILWIS a special NOAA-14 import module (NPR1B) was developed by Gieske and Dost (2000). In this program, adapted from the method by Liping and Rundquist (1994), information from the data's scan line header is used to calibrate the thermal channels 3–5, while the Rao and Chen (1996) method was used to compensate for sensor degradation in the visible channels. The scan line header also contains information on the latitudes and longitudes of each pixels and a first step georeference is made automatically. To compensate for small deviations (a few pixels) a second step final georeference has to be made manually. The NOAA-14 images of the Esfahan area are generally of high quality, because the area's position is close to nadir at satellite overpass. A 1 km resolution is obtained as a matter of routine.

It should be noted that apart from radiometric corrections, no atmospheric corrections are made by NPR1B. It is also necessary to check all images for cloud cover, and discard them if none of the irrigation systems is visible. Details of this procedure can be found in Toomanian et al. (2004). From the original set of 40 images during 1995, only 25 were useful and

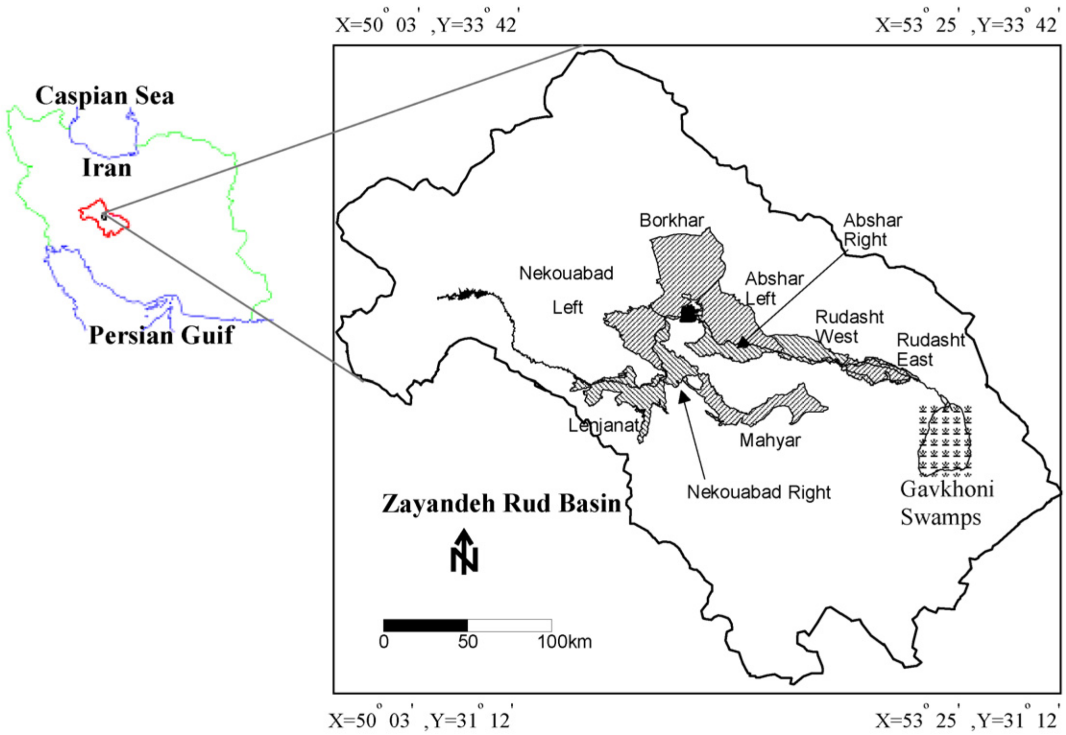

Fig. 1 – Location of study area and major irrigation systems in the Zayandeh Rud Basin, Esfahan, Iran.

used in the study (Table 1). Because cloudy days tend to be more frequent in winter than in summer, the frequency of useful images in summer is higher than in winter.

2.2.1. *Irrigated areas*

Many researchers had established that vegetation indices which are ratios or differences or combination of both, of reflection near infrared and red bands are highly sensitive to crop vigor and crop moisture stress. Out of several vegetation indices, NDVI which is the ratio of difference to sum of reflectance in infrared and red bands is widely used for estimation of irrigated areas (Toomanian et al., 2004). NDVI is a function of green leaf area and biomass and reflective ness of the crop vigor.

2.2.2. *Evapotranspiration*

Evapotranspiration (ET) is the loss of water from open water, soil and plant surface. The ET is governed by the energy and heat exchanges at the land surface. Surface energy balance algorithm for land (SEBAL), (Bastiaanssen et al., 1998), was used to estimate actual and potential evapotranspiration. SEBAL ignoring energy required for photosynthesis and the heat storage in vegetation, in its most simplified form reads as:

$$R_n = G_0 + H + LE \qquad (1)$$

where R_n is the net radiation absorbed at the land surface (W/m^2), G_0 the soil heat flux to warm or cool the soil (W/m^2), H the sensible heat flux to warm or cool the atmosphere (W/m^2) and LE is the latent heat flux associated with evaporation of water from soil, water and vegetation (W/m^2). The applied SEBAL method consists of a physically based one-layer sensible heat transfer scheme and an empirical estimation scheme for soil heat flux. The soil heat flux is computed as an empirical fraction of the net radiation using surface temperature, surface albedo and the normalized vegetation index (NDVI), as the depending variables. The net radiation is computed from spatially variable reflectance and emittance of radiation. A closure of the energy budget on pixel-by-pixel basis is achieved by considering LE as the residual of the energy budget equation. This method requires spectral radiances in the visible, near infrared, and thermal infrared regions of the spectrum to determine its constitutive parameters: surface albedo (α_0), NDVI, and surface temperature (T_0). Net radiation (R_n) is modeled as a sum of incoming and outgoing radiation components. Net short-wave radiation is derived on the basis of astronomical equations together with estimation of atmospheric transmittance (τ_{sw}) and α_0. Incoming long-wave radiation is modeled on the basis of overpass time, air temperatures (T_a) and considered to be constant over the area. Outgoing long-wave radiation is derived with the aid of T_0 and an estimation of the surface emissivity (ε_0) on the basis of NDVI.

In SEBAL method, the initial estimate of surface roughness length for momentum transport (z_{0m}) is based on NDVI using an empirical equation (Moran and Jackson, 1991). Observed wind speed measurements are used to determine the friction velocity (u_*) at each pixel based on the assumption that the wind speed at blending height is aerially constant. Reference heights (Z_1 and Z_2 usually 0.01 and 2.0 m above ground, respectively) are defined as the vertical limits for specifying sensible heat flux (H) and near surface vertical air temperature difference (δT_a). Then, according to the sensible heat transfer equation these limits become applicable for aerodynamic resistance (r_{ah}), (Farah and Bastiaanssen, 2001). By this

Table 1 – Julian day of NOAA images and average normalized difference vegetation index (NDVI) values for the major irrigation systems along the Zayandeh Rud (1995)

Julian day	Abshar Left	Abshar Right	Nekouabad Left	Nekouabad Right
53	0.112	0.137	0.095	0.097
81	0.129	0.161	0.116	0.102
91	0.196	0.237	0.177	0.179
119	0.205	0.280	0.217	0.246
128	0.229	0.298	0.267	0.259
137	0.232	0.297	0.272	0.256
138	0.249	0.306	0.269	0.283
146	0.205	0.241	0.040	0.083
156	0.138	0.143	0.150	0.141
174	0.161	0.199	0.230	0.179
184	0.151	0.168	0.206	0.172
193	0.134	0.152	0.221	0.196
202	0.140	0.166	0.230	0.223
212	0.180	0.243	0.357	0.345
221	0.182	0.224	0.274	0.280
230	0.161	0.215	0.246	0.264
231	0.167	0.238	0.263	0.275
239	0.175	0.227	0.265	0.280
249	0.179	0.240	0.251	0.275
267	0.191	0.250	0.260	0.253
268	0.189	0.255	0.260	0.256
277	0.183	0.230	0.234	0.202
286	0.158	0.211	0.202	0.174
323	0.131	0.142	0.155	0.119
332	0.150	0.157	0.159	0.136

approach the classical problem of the need to estimate $z_{0\,h}$ has been avoided.

The presence of hydrological extremes in the area covered by the image allow for specific solutions of the surface energy balance. By assuming negligible sensible heat fluxes, $R_n = G_0 + LE$ is assigned for wet pixels (low α_0 and T_0, e.g. open water bodies), while for dry pixels (high α_0 and T_0, e.g. extremely dry sandy soils), $R_n = G_0 + H$ is assigned by assuming negligible latent heat fluxes. This implies, $\delta T_{a,wet} = 0$ and $\delta T_{a,dry} = (R_n + G_0)r_{ah}/\rho_a c_p$ and allows for the determination $\delta T_{a,dry}$ using the initial estimate of r_{ah}. In SEBAL it is assumed that δT_a is linearly related to T_0 at all pixels and hence the determination of the relationship is possible with the aid of the extreme pixels. The first estimate of sensible heat flux is thereafter computed and is used to obtain the integrated stability correction using Monin–Obukhov similarity hypothesis. This allows for a second and improved estimation of u_* incorporating the stability correction for buoyancy effect on the momentum flux. The new value of u_* is then used to estimate r_{ah} incorporating the stability correction for heat transport. This procedure is iteratively applied until H converges to the local non-neutral buoyancy conditions for each pixel. The energy balance is finally closed by considering the latent heat flux term as the residue.

The conversion of instantaneous flux values determined above for the satellite overpass time to daily and average monthly evaporation rates is done by the evaporative fraction (Λ), which reads as:

$$\Lambda = \frac{LE}{LE + H} = \frac{LE}{R_n - G_0} \tag{2}$$

The instantaneous evaporative fraction is shown in the literature to be similar to the 24 h evaporative fraction (Shuttleworth et al., 1989; Brutsaert and Chen, 1996), and is used to compute the actual 24 h evaporation from the instantaneous latent heat fluxes:

$$LE_{24} = \Lambda R_{n24} \tag{3}$$

The SEBAL model calculates both the instantaneous and 24 h integrated surface heat fluxes. The latent heat flux represents the energy required for ET, and is computed as the residual of the surface energy balance. The SEBAL model is extensively described elsewhere (Bastiaanssen et al., 1998), and therefore the formulation is not repeated here. Examples of applying SEBAL in other irrigation performance assessment studies are presented in Bastiaanssen et al., 1996, Bastiaanssen, 2000, Chandrapala and Wimalasuriya (2003), Roerink et al. (1997) and Alexandridis et al. (1999).

2.2.3. *Performance indicators*

Irrigation performance indicators have been expressed in terms of efficiencies based on observed flows in different points in the water distribution system. Relative water supply (RWS) as presented by Levine (1982) was expressed as the ratio of total water supply to the total crop-water demand. At the irrigation system level, the total water supply is the total amount of water flowing into the domain from precipitation plus any irrigation supply from diversion. Crop demand is potential evapotranspiration (ET_{pot}) under well-watered conditions. Hence, RWS can be expressed as:

$$RWS = \frac{\text{precipitation} + \text{irrigation}}{ET_{pot}}. \tag{4}$$

It should be noted that, this ratio (RWS) does not reflect whether the crop has received the correct amount of water at the correct time but emphasizes the overall situation of water supply and demand. The ratio does not indicate how effectively the water supply has been utilized.

Water productivity (WP) is more important in water scarce condition and defined as the amount of water used to produce 1 kg of crop. Different WP was identified, based on different definitions of water used. Here we computed $Wp_{\text{process depletion}}$, which refers to the amount of water evapotranspirated to produce 1 kg of crop, by using following expression:

$$WP_{\text{process-depletion}} = \frac{\text{biomass} - \text{production}}{ET_{act}} \tag{5}$$

Where ET_{act} is actual evapotranspiration and considered as beneficial depletion because a plant cannot transpire without having soil evaporation.

The biomass growth rate is related to the energy absorbed by the canopy that was used for carbon dioxide assimilation and computed by the following expression:

$$BGR = 1.04(11.5741K_{24,\text{day}})\int PAR \tag{6}$$

where PAR is the photosynthetically active radiation, W/m^{-2} and $K_{24,\text{day}}$ daily solar radiation, W/m^{-2}.

3. Results and discussion

Since the basic information such as diverted water to irrigation system was not available for all irrigation system, in this paper, attention is focused on the performance of four schemes, namely Nekouabad-Right and Left, and Abshar-Right and Left, which have been in operation since the 1970s. The Borkhar, Mahyar and Rudasht (east and west) systems, parts of which are still under development and have only just begun to benefit from Zayandeh Rud surface irrigation water, have not been included in this analysis.

3.1. *Estimation of irrigated areas*

Based on NDVI data alone it is possible to estimate irrigated area. The results for the NDVI patterns and monthly average for 1995 are shown in Table 1 and Fig. 2, respectively. In general the pattern is clear. The NDVI values rise until May, and then there is a sudden drop, indicating that the winter crops are harvested, after which the values rise again in response to the summer crops. The most important outlier in the series corresponds to NOAA image of day 212.

The time series shows that this image should be corrected or discarded. Probably the deviation is caused by atmospheric conditions, which have not been corrected. There are some distinct differences for the individual irrigation areas, which are briefly discussed below. For an extensive discussion of winter and summer cropping patterns see Sally et al. (2001). Results presented here are based on average NDVI values for the gross command area rather than cropped areas. This makes comparison between systems somewhat difficult.

3.1.1. *Nekouabad*

The pattern is uniform for both Right and Left Bank systems. There is a steep rise in NDVI values and a sudden drop towards the end of May, indicating simultaneous harvesting of all winter crops (mainly wheat and barley) in the system, combined with flooding of areas in preparation for rice planting. After this, NDVI values rise again in response to the growth of the summer crops (mainly rice, corn, potato and onion). The background NDVI of about 0.1 is due to all year crops (orchards and alfalfa). Harvesting of the summer crops takes place more gradually, leading to a steady decline in NDVI values after August.

3.1.2. *Abshar*

The Right Bank system has consistently higher NDVI values than the Left Bank system. This is probably due to the large rock outcrop areas in the Left Bank system. The pattern is similar to that of the Nekouabad system, again with a sharp drop in NDVI values, indicating harvesting of the winter crops. However, NDVI values build up much more slowly for the summer crops and the maximum NDVI values for these crops are lower than for the winter crops. This is probably caused by the relatively more diverse cropping patterns (more corn and vegetables) as compared to the Nekouabad system (where rice is dominant).

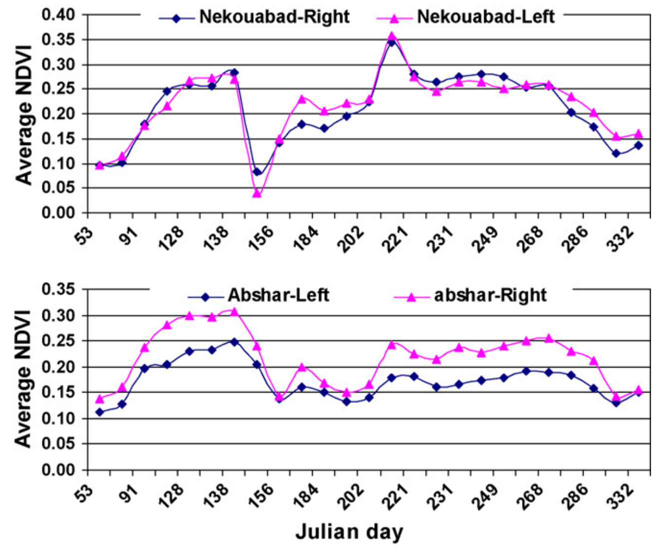

Fig. 2 – Normalized difference vegetation index (NDVI) time curves in major irrigation systems in Zayandeh Rud Basin for 1995.

The results of irrigated areas based on NDVI data for main irrigation systems are summarized in Table 2. With the exception of Nekouabad Left Bank, gross cropped area reported as irrigated and the estimates from NOAA indicate cropped areas are larger than designed, because that there is significant groundwater use that increases the area that can be irrigated. For this reason, use of secondary data alone is insufficient to estimate the actual productivity of the areas, and SEBAL analyses are required to interpret data available from satellites.

3.2. *SEBAL results*

The results from SEBAL for May 1995 are shown in Fig. 3. May represents a transition month with head end areas still having winter crops such as wheat and barley and tail end areas beginning to have summer crops such as rice, fodder and

Table 2 – Irrigated areas measured from maps and estimated from NOAA satellite images for the major irrigation systems along the Zayandeh Rud (1995)

Irrigation system	Designed command area (ha)	Measured command area (ha)	NOAA estimated area (ha)	Estimated cropping intensity (%)
Nekouabad-Right Bank	13,500	20,532	16,631	81
Nekouabad-Left Bank	48,000	38,863	30,313	78
Abshar-Left Bank	15,000	52,370	38,754	74
Abshar-Right Bank	15,000	22,565	16,247	72

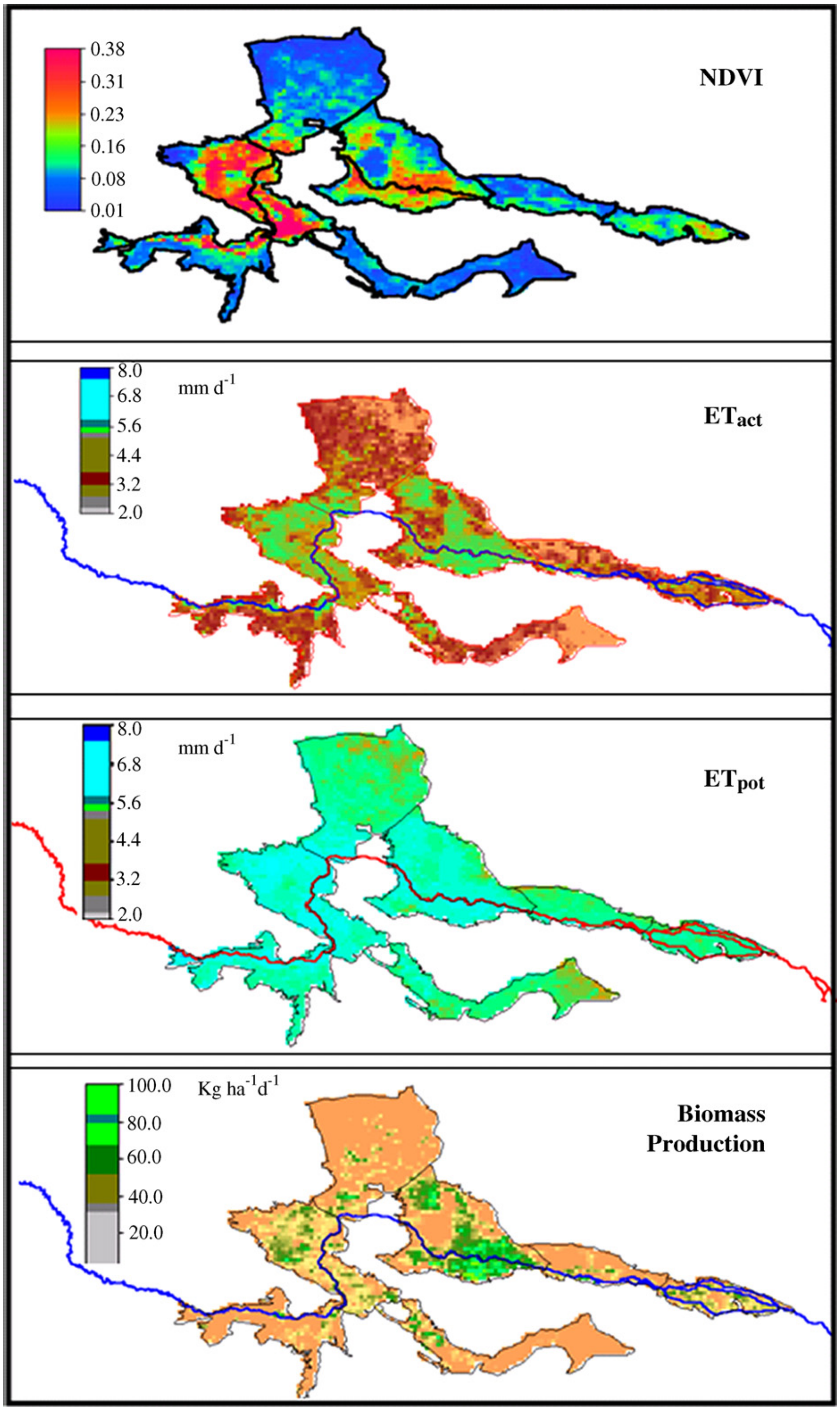

Fig. 3 – Result of normalized difference vegetation index (NDVI), actual evapotranspiration (ET_{act}), potential evapotranspiration (ET_{pot}) and biomass production using surface energy balance algorithm for land (SEBAL) analyses in Zayandeh Rud Basin for May 1995.

maize. Irrigated areas can be clearly distinguished from the NDVI map with values of 0.20 and higher. This value of NDVI for crops is rather low, and can be explained by low cropping intensity, with a high degree of fallow within an individual pixel at the time of image acquisition. High intensities can be found for the Abshar systems, reflecting the dominant cropping pattern with mainly winter crops. Interesting are also the relatively high intensities for the Rudasht-East system, indicating that during spring a reasonable amount of water is reaching this downstream area.

3.2.1. Monthly variation in irrigation performance

Monthly average variation of NDVI values for the four main systems are shown in Fig. 4. As mention before, the dual cropping pattern can be observed with high NDVI values from March to May and from August to October. Lower values in June and July are the result of the end of the growing season for spring crops (wheat) and the start of the summer crops (rice). For Abshar-Right, and especially Abshar-Left, the peak for summer crops is lower as a result of the smaller area cultivated with rice.

The results of ET_{pot} show a similar pattern for all systems (Fig. 4) and are quite constant over the area with peak values for mid-summer around 8 mm day^{-1} in May. Spatial variation of ET_{pot} with the value around 7 mm day^{-1} over the irrigated systems as variability in the prevailing weather conditions is low (Fig. 3). Some lower values can be seen for the mountainous areas north of Abshar-Left as temperatures are lower resulting in lower ET_{pot}. As described before, SEBAL is based on the energy balance where sensible heat flux is related to temperature. However, for hill-sloops surface temperatures can deviate substantially from the equivalent temperature for flat areas, and so the SEBAL results are unreliable for undulating areas. Therefore, the analyses will be only focusing on the flat irrigated areas.

Values of ET_{act} showed the same trend as NDVI levels in the irrigated systems (Fig. 4). High NDVI values correspond to high ET_{act}. The spatial variation in actual evapotranspiration is presented in Fig. 3. The bends of the river are clearly visible from the higher ET_{act}. The values of ET_{act} vary from 0 to 5.6 mm day^{-1}. However, ET_{act} from irrigated surfaces and bare soil was found about the potential rate and near the zero, respectively. At this time of image, the Nekouabad and Abshar systems still have winter crops such as wheat and barley and show the higher value of ET_{act} but tail end areas beginning to preparation for summer crops and have a lowest evaporation. Monthly results of ET_{act} (Fig. 4) reflects again clearly the difference between the Nekouabad and the Abshar systems, with the latter one having a cropping pattern existing mainly out of winter crops harvested in June, while Nekouabad system has sufficient water to allow good crop growth throughout the summer.

The estimated crop productions can be considered as the integrating parameter of water and crop management. The

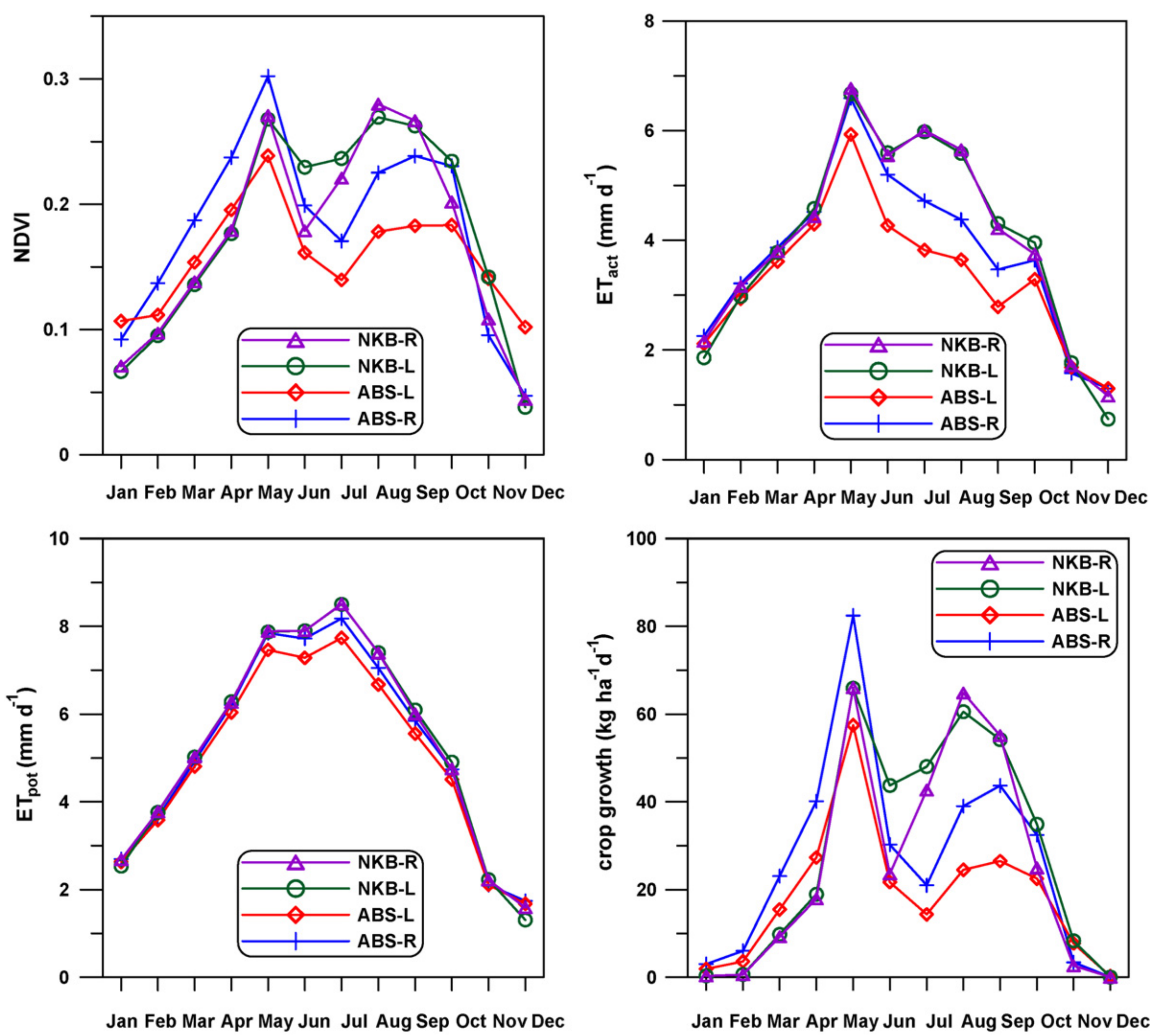

Fig. 4 – Monthly values of normalized difference vegetation index (NDVI), actual evapotranspiration (ET_{act}), potential evapotranspiration (ET_{pot}) and biomass production for Nekouabad-Right Bank (NKB-R), Nekouabad-Left Bank (NKB-L), Abshar-Right Bank (ABS-R) and Abshar-Left Bank (ABS-L) irrigation systems in Zayandeh Rud Basin (1995).

spatial variation of biomass production (Fig. 3) shows clearly that the Abshar system is the most productive system in May, with daily biomass production values for some areas of 100 kg ha^{-1} day^{-1}. For a crop with an active growing period of 120 days this translates to 12,000 kg ha^{-1} biomass. The conversion factors from biomass to harvested product depends on crop, variety, and plant physiological condition, and values ranges from 10 to 30%, resulting in a actual yield of 1200–3600 kg ha^{-1}. Monthly values of biomass production showed the same trend as NDVI and ET_{act} levels in the all systems (Fig. 4), high biomass values correspond to high NDVI and ET_{act}. The peaks values happened in May when climatic conditions in terms of radiation are optimal and sufficient water is available from precipitation, soil moisture storage, and irrigation.

3.2.1.1. *Monthly variation of relative water supply*. Data for the water diversions into each of the main irrigation networks were obtained from the provincial office of the ministry of energy. Fig. 5 shows the theoretical water availability in the major irrigation systems in the Zayandeh Rud, based on their respective design irrigation command areas. It will be observed that the average availability of water in the Nekouabad Left Bank system (about 3 mm day^{-1}) is less than that in the other systems (more than 4 mm day^{-1}). The much larger design command area of Nekouabad Left Bank (48,000 ha) could be one reason for this. Fig. 5; indicate clearly that there are three separate water delivery conditions. From January to March, hardly any water is issued to any system. Water releases increase significantly from April onwards and peak releases occur between May and September, coinciding with the hottest and driest part of the year. From October to December water deliveries are at an intermediate level, reflecting the need for continued irrigation for some crops but at a lower level.

While water supply information was readily available, the estimation of water demand proved to be more difficult due to the absence of data on irrigated areas and cropping patterns. To overcome this difficulty, this information was finally derived from the available district-level agricultural statistics for Esfahan province. But these data cover all crops and are not specifically focused on the irrigation systems. Hence, a simple spreadsheet-based model was devised to derive the required

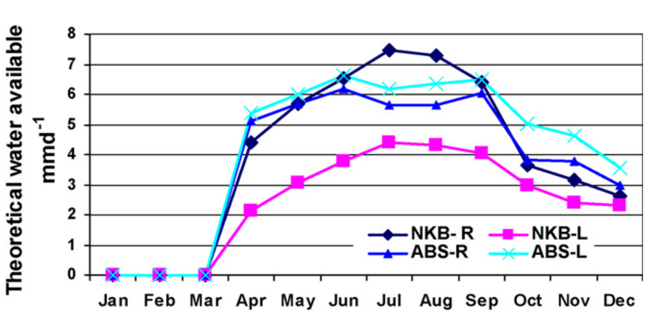

Fig. 5 – Theoretical water availability in the Nekouabad-Right Bank (NKB-R), Nekouabad-Left Bank (NKB-L), Abshar-Right Bank (ABS-R) and Abshar-Left Bank (ABS-L) irrigation systems in the Zayandeh Rud Basin, based on their respective design irrigation command areas (1995).

information on irrigated areas from available records. This approach yielded credible results with far less time and effort compared to aggregating village-level data. But the validity of this approach has to be further verified against satellite image-based estimates of irrigated areas (more detail can be find in Sally et al., 2001). The water demand for selected irrigation system was obtained from irrigated area and ET_{pot}.

Monthly values of precipitation, ET_{pot} and water supply for the four irrigation systems in Zayandeh Rud Basin are shown in Fig. 6. The results of irrigation supply and demand indicate that in all the four systems studied, although the water deliveries show an increasing trend almost reflecting the increasing demand from January to about June, the supply actually falls short of demand. In the remaining 6 months of the year, there appears to be a phenomenon of 'over-correction', generally resulting in surpluses of RWS. In all the systems studied, the water supply exceeds demand (RWS more than 1), from October to December. The largest deficits (RWS less than 1) occur between February and May.

Abshar-Right Bank receives the largest RWS. This is especially so during summer when the water releases are far in excess of the needs of the actual cropping pattern; the areas actually cropped are less than the design area, on which the water releases to the systems are based. On the other hand, the Abshar left bank system shows an opposite trend. It has the largest deficits and the smallest RWS when compared to the other systems in a given period. The actual cropped areas in this system are much more than the design command area. As the irrigation releases are based on the design area this will naturally result in deficits. Similarly, the Nekouabad-Right and Left Bank systems have large extents of rice, cultivated from May to September. But both systems have deficits in surface water at the start of the cropping season.

3.3. *Annual variation in irrigation performance*

The results for four irrigation systems were aggregated to annual totals crop areas (Table 3) by taking the maximum NDVI value for each pixel in April and September and assuming that all values higher than 0.2 were cropped.

Releases for irrigation differ substantially from system to system. Figures presented here relate to the whole system area, rather than the areas served by surface irrigation. Converting these values to the official command areas leads to application rates between 1000 and 1500 mm ha^{-1}. Precipitation was considered to be similar for all areas, as distance between systems was limited. Because precipitation is low throughout the area, it has relatively little impact on annual water balance.

The overall water balances for the systems are not closed (Table 3) and three of the four systems show a water deficit. The apparent water surplus for Nekouabad-Left Bank can be explained by the new offtake canal from Nekouabad-Left bank main canal to the new Borkhar system. It is unclear how much water was actually delivered to Borkhar, so the water supply to Nekouabat-Left only could not be determined.

The other water in the three water deficit systems can be supplied from two water resources. First of all, a certain amount of water is extracted directly from the river, which is not included in the water balance. Second, groundwater

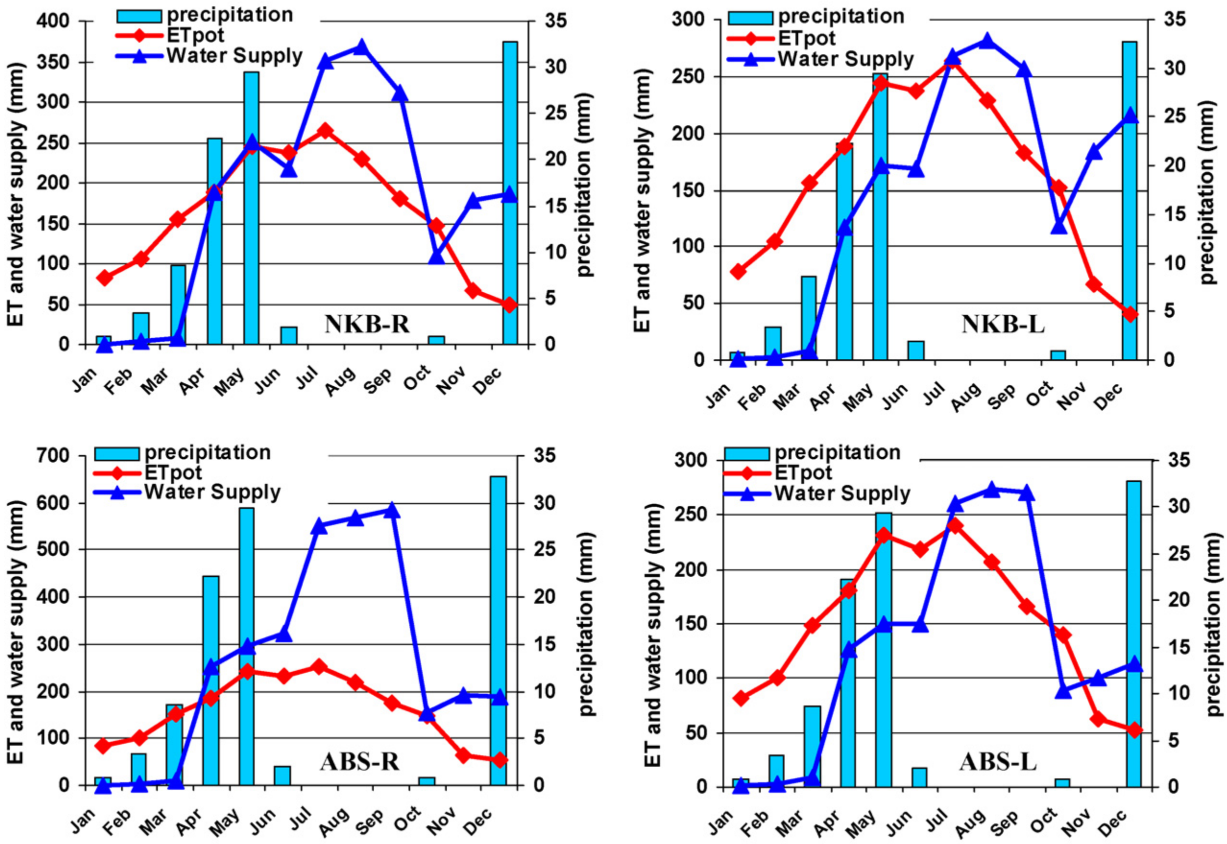

Fig. 6 – Monthly values of precipitation, potential evapotranspiration (ET_{pot}) and water supply for the Nekouabad-Right Bank (NKB-R), Nekouabad-Left Bank (NKB-L), Abshar-Right Bank (ABS-R) and Abshar-Left Bank (ABS-L) irrigation systems in the Zayandeh Rud Basin (1995).

irrigation is extensively applied in the area and recharge by river or other resources. spatial and temporal analysis of ground water data provided from the ministry of energy on monthly observations from 717 wells over a 10 years period show that the recharge of groundwater, either from the Zayandeh Rud or from irrigation systems, is quite apparent. Few areas close to the river show water table declines of more than 10 m over the 10 years period, but areas away from the river show substantial decline, notably in Mahyar, Nekouabad-Left and Right Banks, and in Borkhar. A change of over 1 m per year implies that at least 100 mm of water has been extracted each year in excess of natural recharge (more detail can be find in Droogers and Miranzadeh, 2001). Quantitative information about these two additional inputs in the systems is lacking, but can be estimated as the missing term in the water balance. For Abshar-Left this combined groundwater and unofficial water extraction is about 190 mm (Table 3). The designed command area of Abshar-Left is 15,000 ha, while the cropped area as determined by NOAA is almost 39,000 ha. It is clear that the additional areas are irrigated by groundwater. Nekouabad-Right and Abshar-Right show an annual deficit of 178 and 74 mm, respectively. Designed command area for these systems are 13,500 and 15,000 ha, while actual cropped areas are higher (Table 3).

Comparison between the results from current study and supply and demand study (Sally et al., 2001) are shown in

Table 3 – Annual water balance and water productivity (biomass production/actual evapotranspiration) in major irrigation systems in the Zayandeh Rud Basin (1995)

Irrigation system	ET_{act} [a]	Irrigation (mm)	Precipitation (mm)	Balance (mm)	Biomass (kg ha^{-1})	WP_{depl} [b] (kg m^{-3})
Nekouabad Right Bank	1183	882	123	−178	9388	0.79
Nekouabad Left Bank	1180	1227	123	170	10528	0.89
Abshar Left Bank	924	439	123	−362	6806	0.74
Abshar Right Bank	1088	891	123	−74	9894	0.91

[a] Actual evapotranspiration (ET_{act}).
[b] Water productivity of process depletion (WP_{depl}).

Table 4 – Comparison between the water balance in current study (NOAA) and supply and demand study based on Cropwat and cropping patterns, in major irrigation systems in the Zayandeh Rud Basin (1995)

Irrigation system	NOAA (mm)	Accounting (mm)
Nekouabad Right Bank	−178	166
Nekouabad Left Bank	170	170
Abshar Left Bank	−362	−141
Abshar Right Bank	−74	332

Table 4. In general the supply and demand study resulted in lower deficits, which is somewhat unexpected as potential ET (Cropwat) was used, rather than actual ET. On the other hand, the supply and demand study was based on reported cropped areas, which might be lower than the actual cropped areas. Obviously, NOAA is based on the real irrigated area. Further analysis should be done to compare the results of the two studies.

Finally, the results of current study can be used to explore the water productivity of the systems. As described before we used the water productivity, expressed as the biomass production over the amount of water depleted by ETact. Abshar-Left appears to be the least productive of the four systems. Groundwater quality in the Zayandeh Rud is much poorer than surface water (see Salemi et al., 2000), so for Abshar-Left, with its high percentage groundwater irrigation, this WP is low. For Nekouabad-Left, with limited groundwater irrigation, WP is high. Although groundwater extraction seems high for Abshar-Right, WP is not low. Probably, the negative values in the water balance for this system are mainly caused by unaccounted water extraction from the river rather than from groundwater.

4. Conclusions

The application of satellite remote sensing has matured largely over the past decades, and can bring practical results already. The basic parameters such as RWS, vegetation indices, ET_{pot}, ET_{act} and WP are already standard products that are used widely in the monitoring irrigation performance by remote sensing. Many irrigation systems in world have already been under investigation for irrigation performance by remote sensing with satisfactory levels. Actual developments are especially oriented towards more automatic processing of the models while keeping actual accuracy levels. Time series of ET_{act} are now emerging as important combined temporal and spatial analysis tools for actual crops water consumption. Assessment of irrigation performance is largely benefiting from such advancements of the remote sensing science.

The SEBAL methodology has been applied to estimate actual and potential evapotranspiration over a mixed vegetation canopy at irrigation system in Zayandeh Rud Basin of Iran, in 1995. Estimates of ET were obtained using the time-series NOAA–AVHRR images. Satellite data was supplemented by ground data consisting of air temperature and wind speed from the meteorological stations at satellite overpass time and solar radiation data. Potential and actual evapotranspiration in the basin for the total 12-month period was estimated at 1375 mm with a range between 1209 and 1474 mm.

The accuracy and validity of the SEBAL method has been demonstrated extensively (e.g. Bastiaanssen, 2000). The observed problems in undulating areas require more work, but as we have used only results from the flat irrigated areas, this does not interfere with the results presented. Estimates for cropped area have been derived by using a fixed threshold value for the NDVI. A more accurate method is presented by Toomanian et al. (2004), but deviations appeared to be small.

This device provides the potential for practical application of remote sensing approaches to basin scale water balance studies by giving area wise averaged ET estimates over a large area.

The main advantage of the methodology described here over the more traditional assessment methods is that the water balance of an entire system is considered. The traditional performance assessments use only the "official" areas and water extractions, resulting in biased conclusions. In many irrigation systems, the unofficial water users contribute substantially to the performance of the whole system, as they often rely on runoff or percolation losses from the "official" users, by using drain water or groundwater. In the methodology described here no distinction has to be made between these two groups and the entire system performance is assessed.

Results from this study can be used as a strategic decision support system (S-DSS); results from the past have been used to analyze the performance of the systems and can be used to make strategic decisions to improve this performance. Besides this S-DSS, the same methodology can be used in an operational mode (O-DSS) where real time data acquiring can be used to make day-to-day decisions how to operate the scarce water resources. Such an approach is already semi-operational in some countries such as Sri Lanka and The Netherlands.

REFERENCES

Alexandridis, T., Asif, S., Ali, S., 1999. Water performance indicators using satellite imagery for the Fordwah Eastern Sadiqia (South) Irrigation and Drainage Project. Sensing data. IWMI Pakistan Research Report R-87. International Water Management Institute, Sri Lanka.

Bandara, K.M.P.S., 2003. Monitoring irrigation performance in Sri Lanka with high-frequency satellite measurements during the dry season. J. Agr. Water Manage. 58, 159–170.

Bastiaanssen, W.G.M., 2000. SEBAL based sensible and latent heat flux in the irrigated Gediz Basin, Turkey. J. Hydrol. 229, 87–100.

Bastiaanssen, W.G.M., Menenti, M., Feddes, R.A., Holtslag, A.A.M., 1998. A remote sensing surface energy balance algorithm for land (SEBAL), 1. Formulation. J. Hydrol. 212–213, 198–212.

Bastiaanssen, W.G.M., van der Wal, T., Visser, T.N.M., 1996. Diagnosis of regional evaporation by remote sensing to support irrigation performance assessment. Irrig. Drain. Syst. 10, 1–23.

Bos, M.G., 1997. Performance indicators for irrigation and drainage. Irrig. Drain. Syst. 11, 119–137.

Brutsaert, W., Chen, D., 1996. Diurnal variation of surface fluxes during thorough drying (or severe drought) of natural prairie. Water Resour. Res. 32 (7), 2013–2019.

Chandrapala, L., Wimalasuriya, M., 2003. Satellite measurement supplemented with meteorological data to operationally estimate actual evaporation of Sri Lanka. J. Agr. Water Manage. 58, 89–107.

Chemin, Y., Platonoy, A., Ul-Hassan, M., Abdullaey, I., 2004. Using remote sensing data for water depletion assessment at administrative and irrigation system levels. J. Agr. Water Manage. 64 (3), 183–196.

Choudhury, B.J.M., 1997. Global patterns of potential evaporation calculated from the Penman–Monteith equation using satellite and assimilated data. Remote Sens. Environ. 61, 64–81.

Droogers, P., Kite, G., 1999. Water productivity from integrated basin modelling. Irrig. Drain. Syst. 13, 275–290.

Droogers, P., Kite, G., 2001. Simulation modelling at different scales to evaluate the productivity of water. Phys. Chem. Earth 26 (11–12), 877–880.

Droogers, P., Miranzadeh, M., 2001. Spatial analysis of groundwater trends: example for Zayandeh Rud Basin, Iran. IAERI-IWMI Research Reports 9.

Farah, H.O., Bastiaanssen, W.G.M., 2001. Impact of spatial variations of land surface parameters on regional evaporation: a case study with remote sensing data. Hydrol. Process. 15, 1585–1607.

Gieske, A., Dost, R., 2000. NPR1B. In: NOAA-14 Import into ILWIS, ITC Shareware, Enschede, The Netherlands.

Levine, G., 1982. Relative Water Supply: An Explanatory Variable for Irrigation Systems. Technical Report No. 6. Cornell University, Ithaca, NY, USA.

Liping, D., Rundquist, D.C., 1994. A one-step algorithm for correction and calibration of AVHRR level 1b data. Photogramm. Eng. Rem. Sens. 60, 165–171.

Menenti, M., Azzali, S., 1992. The role of remote sensing, geographic information system and models in the management of large irrigation schemes. In: Singh, R.B. (Ed.), Environmental Monitoring, Application of Remote Sensing and GIS. Geocarti International Centre, Hong Kong, pp. 73–89.

Molden, D., Sakthivadivel, R., 1999. Water accounting to assess use and productivity of water. Water Resour. Dev. 15, 55–71.

Moran, S.M., Jackson, R.D., 1991. Assessing the spatial distribution of evaporation using remotely sensed inputs. J. Environ. Qual. 20, 725–737.

Murray-Rust, H., Sally, H., Salemi, H.R., Mamanpoush, A., 2000. An overview of the hydrology of the Zayandeh Rud Basin. IAERI-IWMI Research Reports 3.

Nieuwenhuis, G.J.A., Smidt, E.M., Thunnissen, H.A.M., 1985. Estimation of regional evapotranspiration of arable crops from thermal infrared images. Int. J. Remote Sens. 6 (8), 1319–1334.

Pelgrum, H., Bastiaanssen, W.G.M., 1996. An inter-comparison of techniques to determine the area-averaged latent heat flux from individual in situ observations: a remote sensing approach using the European Field Experiment in a desertification-threatened area data. Water Res. 32 (9), 2775–2786.

Rao, C.R.N., Chen, J., 1996. Post-launch calibration of the visible and near-infrared channels of the advanced very high resolution radiometer on the NOAA-14 spacecraft. Int. J. Remote Sens. 17 (14), 2743–2747.

Roerink, G.J., Bastiaanssen, W.G.M., Chambouleyron, J., Menenti, M., 1997. Relating crop water consumption to irrigation water supply by remote sensing. Water Resour. Manage. 11 (6), 445–465.

Salemi, H.R., Mamanpoush, A., Miranzadhe, M., Akbari, M., Torabi, M., Toomanian, N., Murray-Rust, H., Droogers, P., Sally, H., Gieske, A., 2000. Water Management for Sustainable Irrigated Agriculture in the Zayandeh Rud Basin, Esfahan Province, Iran. IAERI-IWMI Research Reports 1.

Sally, H., Murray-Rust, H., Mamanpoush, A.R., Akbari, M., 2001. Water supply and demand in four major irrigation systems in the Zayandeh Rud Basin, Iran. IAERI-IWMI Research Reports 8.

Seckler, D., Barker, R., Amarasinghe, U., 1999. Water scarcity in the twenty-first century. Water Resour. Dev. 15, 29–42.

Shuttleworth, W.J., Gurney, R.J., Hsu, A.Y., Ormsby, J.P., 1989. FIFE: the variation in energy partitioning at surface flux sites, remote sensing and large-scale global processes. In: Proc. Baltimore Symp., IAHS Red Book Series, vol. 186. pp. 67–74.

Toomanian, A., Gieske, A., Akbari, M., 2004. Irrigated area determination by NDVI-Landsat upscaling techniques, Zayandeh River Basin, Esfahan, Iran. Int. J. Remote Sens. 15 (22), 4945–4960.